

thetic methods of fundamental importance in organosilicon chemistry and also SQ functionalization, mediated by easily available Pt-based Karstedt or Speier catalysts.^{22,23} Even though this process is burdened with inconvenience, *i.e.* selectivity and formation of by-products (derived from side processes, *e.g.* dehydrogenative silylation, isomerization, or olefin hydrogenation), it is a convenient route to obtain compounds of desirable physical and chemical properties.^{24,25}

The concept of linear co-polymeric SQ-based systems, so-called Beads on a Chain (BoC) polymers, *i.e.* linear co-polymers with DDSQ fragments embedded in the polymer chain, is known.^{26,27} The methods of their formation included various reactions, *i.e.* cross-metathesis, silylative coupling, Piers-Rubinsztajn, or other types of condensation reactions.^{26–34} However, the number of reports on these copolymeric DDSQ-based systems is still limited, especially concerning hydrosilylation.^{28,31,35} Due to growing attention towards the interesting physical properties of these new materials, *i.e.* thermal (also insulating) and mechanical parameter enhancement, the transmittance of the prepared films, hydrophobic character, *etc.*, an increase in the development of methodologies using varied comonomers to obtain new systems of tailored properties is observed.^{36–41}

In this paper, we focus on the studies on Pt-catalysed hydrosilylation reactions using divinyl/dihydro-substituted double-decker silsesquioxanes to verify the impact of the placement of Functional Groups (FGs), *i.e.* Si–H and Si–HC=CH₂ on the reactivity of these systems. A novel, molecular DDSQ-based compound was disclosed, possessing an additional –OSi(Me₂)– linker between the Si–O–Si core and Si–HC=CH₂. The versatility of the hydrosilylation procedure, elaborated for the synthesis of molecular compounds, was applied to obtain linear, macromolecular co-polymers with diorganosilicon fragments and the DDSQ-unit embedded in the main chain of the linear polymer. The possibility to introduce different diorganosilicon co-monomers and the presence of additional –OSi(Me₂)– fragments were used to demonstrate and study their influence on the thermal, mechanical, and hydrophobic properties of the resulting DDSQ-based macromolecular systems.

Results and discussion

Our group has reported on the chemistry of double-decker silsesquioxanes with vinyl reactive groups that are susceptible to silylative coupling (SC) and cross-metathesis (CM) reactions leading to molecular and linear macromolecular compounds (depending on the number of vinyl moieties in the olefin reagent).^{19,30,42} Additionally, Si–H functionalized double-decker SQs are active in the hydrosilylation (HS) of arenes also resulting in analogous molecular and macromolecular DDSQ-based systems.^{28,31,35} Linear macromolecular compounds may be described as co-oligomers with DDSQ fragments embedded between the aryl moieties by an unsaturated ethenyl-bridge when SC/CM is used or a saturated ethyl-bridge when HS is applied for their syntheses. Encouraged by our previous

research on the synthesis of double-decker SQ-based arene derivatives of molecular and macromolecular architecture *via* hydrosilylation, we decided to study this more comprehensively.³¹ Our goal was to verify the reactivity of Si–HC=CH₂ and Si–H difunctionalized DDSQ in hydrosilylation and apply them as reagents in the abovementioned reaction with dihydro- or divinyl-substituted organosilicon compounds, respectively.

The DDSQ-based reagents used in the studies, *i.e.* DDSQ-2SiH (**1a**) and DDSQ-2SiVi (**1b**) are well known, but we succeeded in obtaining the crystal structure of **1b** for the first time (Fig. 1).^{19,31} For our studies, we also applied a novel DDSQ derivative possessing an additional –OSi(Me₂)– linker between the Si–O–Si core and the –HC=CH₂ functionality (DDSQ-2OSiVi (**1c**)). It was obtained in a hydrolytic condensation reaction of 9,19-dihydroxy-octaphenylsilsesquioxane⁴³ with chlorodimethyl-vinylsilane in a high yield (94%) and characterized by ¹H, ¹³C, ²⁹Si NMR, and FT-IR spectroscopy. Its structure was also confirmed by XRD for crystals obtained in MeCN during a slow (approx. two weeks) crystallization process (Fig. 1). Fig. 1 shows the perspective view of molecules **1b** and **1c**.

The crystal structures unambiguously confirm the proposed reaction products. The values of the geometrical parameters (bond lengths, angles) are very consistent and close to the typical bond lengths and angles in similar compounds. The structures are quite regular – the mean values of Si–O bonds are 1.617(1) Å in **1b** and 1.616(1) Å in **1c**, and the Si–O–Si angles are within a relatively (as compared with similar structures) narrow range, 144.10(9)°–163.31(9)° in **1b**, and 139.3(2)°–162.5(2)° in **1c**. Molecule **1b** is C_i-symmetrical, and it lies across the inversion centre in the space group P2₁/c. In turn, the main molecule **1c** skeleton (silsesquioxane cage) is only in good approximation C_i-symmetrical; the disposition of phenyl rings breaks the symmetry and lowers it to C₁. The crystal architectures are determined mainly by weak van der Waals interactions.

Interestingly, the XRD analysis of **1c** revealed the formation of only a *cis*-geometry (Fig. 2) which may suggest different sus-



Fig. 1 Perspective view of the compound **1b** (left) and **1c** (right); ellipsoids are drawn at the 50% probability level, hydrogen atoms are shown as spheres of arbitrary radii. For **1b** only the higher-occupied part of the disordered fragment is shown.



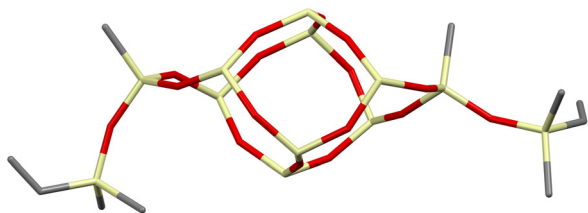


Fig. 2 Perspective view of compound **1c**; phenyl rings and hydrogen atoms are omitted to visualize the bare Si–O–Si DDSQ core.

ceptibility forms of *cis*- and *trans*-isomers, as both were obtained in the reaction (see ^{29}Si NMR in the ESI, p. S-9†). It requires diverse procedures for their separation.⁴⁴ This may also suggest that the presence of an –OSi(Me₂)– bridge may affect the physical properties of this compound which in turn may alter the properties of its follow-up derivatives.

Initially, we studied hydrosilylation in two model reactions differing in the architecture of DDSQs, *i.e.* by varying the placement of the reactive Si–H moiety (**1a** or **2-H**) vs. Si–HC=CH₂ (**1b**, **1c** or **2-Vi**) in hydrosilylation reagents as presented in Scheme 1.

The model reactions were carried out using real-time *in situ* FT-IR measurements (see the ESI†) to establish the time required for the complete conversion of Si–H bonds (based on changes in the surface area of the band at $\bar{\nu} = 895\text{ cm}^{-1}$ characteristics for stretching vibrations of Si–H bonds) in the HS process to yield molecular DDSQ-based difunctionalized compounds. The catalyst used for this purpose is commercially available and it is still widely applied Pt-Karstedt's catalyst ([Pt₂(dvds)₃] in 10^{−4} mol of Pt loading per mol of Si–H group. The reagent stoichiometry was maintained equivalent. We noted previously, that alkene excess may affect the reaction time but mainly its initial time and does not significantly reduce the total reaction time.¹⁶ However, the reaction conditions of these model reactions were to be applied in further copolymerization HS which is why the equimolar reagent stoichiometry was crucial. Hydrosilylation (besides possible side reactions) is generally selective towards the β-anti-Markovnikov addition product but the α-product may also occur. It should be emphasized that in our case, as previously noted, the process was regioselective towards the formation of β-hydrosilylation products (for details see the ESI†). As a result, two types of products differing in the presence of an additional –OSi(Me₂)– linker between the Si–O–Si core and the SiMe₂Ph substituent were formed (for $m = 0$, **3a-Vi**, **3b-H**; $m = 1$, **3c-H**). The reaction profiles of the hydrosilylation progress for the model reaction are presented in Fig. 3.

As shown in Fig. 3, rapid reagent conversion appeared within the first 10–40 min after [Pt₂(dvds)₃] addition (up to 50% of Si–H consumption). However, the real times of the reaction estimated by *in situ* FT-IR are as follows: 48 min for **1a**, 290 min for **1b**, and 120 min for **1c**. The higher reactivity of **1a** may be explained by the presence of D-type functional Si–H in its structure. The presence of vinyl moieties in **1b** and **1c** changes the electronic



Scheme 1 Model reactions for the hydrosilylation using organosilicon compounds with different locations of the Si–H functionality.

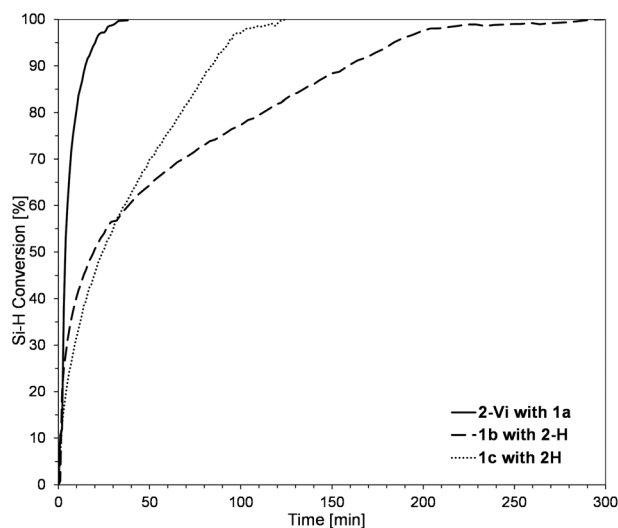


Fig. 3 Reaction profile for the hydrosilylation of **2-Vi** with **1a** and **1b**, **1c** with **2-H** determined by real-time *in situ* FT-IR spectroscopy. [Pt₂(dvds)₃] × 10^{−4} per mol of Si–H, equimolar stoichiometry of Si–H and Si–HC=CH₂ reagents, toluene ($m_{\text{SQ}}/V_{\text{tot}} = 33\text{ mg mL}^{-1}$), 95 °C.

properties of these reagents and lowers the reactivity of **1b** with the D-type functional Si–HC=CH₂ group may when compared with **1c** – M-type of Si–HC=CH₂. It may be noted that the electron-withdrawing effect of the oxygen atom(s) present in the surrounding of the reactive Si–H (in **1a**) promotes its reactivity but decreases the reactivity of Si–HC=CH₂ (in **1b** and **1c**). These observations are in accordance with the Chalk–Harrod HS mechanism.²² The conclusions derived from these model reactions were applied in further copolymerization HS and albeit the structures of the obtained products for $m = 0$ **3a-Vi** = **3b-H** are structurally equal, the reagents built and reaction times varied along with different reaction profiles. We decided to conduct them as a studied model to observe if the electronic and steric effects of Si–H and Si–HC=CH₂ placement in DDSQ substrates affect the formation of copolymeric products.



In the next stage of our studies, we transferred the information obtained from model reactions and performed copolymerization *via* hydrosilylation of **1b** and **1c** with a series of dihydrosubstituted (**5d–h**) organosilicon compounds and divinyl- (**4d–g**) organosilicon compounds with **1a** derivative. In all tests, the reaction conditions were maintained the same, *i.e.* 10^{-3} mol of Pt-Karstedt's catalyst loading per mol of Si–H group, toluene ($m_{1a}/V_{\text{tol}} = 33 \text{ mg mL}^{-1}$), and an equimolar stoichiometry of Si–H and Si–HC=CH₂ reagents (*e.g.* [**1a**]:[**4d**] = 1:1), 95 °C and 24 h (or 72 h when noted). The overview of this process that leads to the organic–inorganic co-oligomers with DDSQ in the main chain is presented in Scheme 2.

The model reactions enabled hydrosilylation oligomerization reactions under optimized reaction conditions. After several tests, a series of co-oligomeric products with DDSQ fragments with organosilicon spacers differing in the presence (**7c(d–h)**)/absence (**6a(d–g) = 7b(d–g)**) of an additional –OSi(Me₂)– linker between the DDSQ core and the organosilicon spacer was obtained. It is worth noting that hydrosilylation of **4d–g** with **1a** and **1b** with **5d–g** leads to products of analogous structure, *i.e.* of the identical architecture of mers and **6a(d–g)** may be denoted as **7b(d–g)** (Scheme 2). Nevertheless, they will be mentioned separately, to point out the differences in the degree of co-polymerization depending on the placement of the functional Si–H/Si–HC=CH₂ moiety in DDSQs (**1a** or **1b**) and their reactivity in the hydrosilylation.

The obtained co-oligomers were purified by precipitation in methanol or *n*-hexane (with the eventual addition of water) and subsequent decantation (if possible), dried under reduced pressure to afford solids **6a(d–g)** or viscous solids (waxes) **7c(d–h)**. Due to the possibility of solvent occlusion which was anticipated based on the product's chain structure and degree of viscosity, it should be advised to dry them under a vacuum with the use of liquid nitrogen. Isolated compounds were analysed by NMR and FT-IR spectroscopy to confirm their structures. The prepared co-oligomers were subjected to Gel Permeation Chromatography (GPC) to measure their molecular weights

Table 1 Molecular weights of co-polymers obtained *via* hydrosilylation of divinyl-substituted organosilicon derivatives (**4d**, **4f**, and **4g**) with dihydro-substituted DDSQ (**1a**)

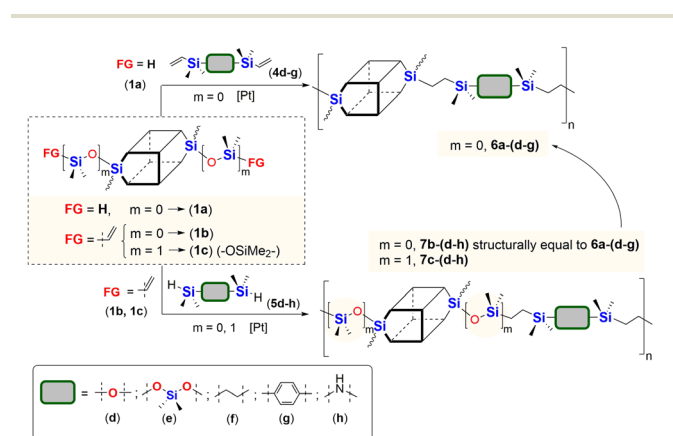
| Entry | Sample | All fractions | | | | |
|-------|---------------------------------|---------------|---------------------------------|---------------------------------|-----|-----------------|
| | | | M_w (g mol ⁻¹) | M_n (g mol ⁻¹) | D | DP _n |
| 1 | 6a–d–24h | | 6500 | 4500 | 1.4 | 4 |
| 2 | 6a–d–72h | | 7200 | 4900 | 1.5 | 4 |
| 3 | 6a–d–24h PtO₂ | (d) | 6100 | 4300 | 1.4 | 3 |
| 4 | 6a–f–24h | | 7700 | 5200 | 1.5 | 4 |
| 5 | 6a–f–72h | | 12 300 | 6900 | 1.8 | 5 |
| 6 | 6a–f–24h PtO₂ | (f) | 6500 | 4700 | 1.4 | 3 |
| 7 | 6a–g–24h | | 22 800 | 9500 | 2.4 | 7 |
| 8 | 6a–g–72h | | 26 300 | 10 000 | 2.6 | 7 |
| 9 | 6a–g–24h PtO₂ | (g) | 13 800 | 7300 | 1.9 | 5 |

Reaction conditions: [Pt₂(dvds)₃] and PtO₂ – 10^{-3} per mol of Si–H, equimolar stoichiometry of Si–H and Si–HC=CH₂ reagents, *e.g.* [**1a**]:[**4d**] = 1:1, toluene ($m_{1a}/V_{\text{tol}} = 33 \text{ mg mL}^{-1}$), 95 °C. D = dispersity index, DP_n = degree of polymerization.

and polydispersity indexes. The measured M_n , M_w , and D values are presented in Tables 1 and 2.

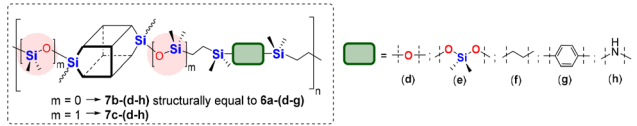
Tests verifying the reactivity of functional DDSQs by using **1a** (with reactive Si–H moiety) in a hydrosilylation reaction using divinylsubstituted organosilicon derivatives (**4d**, **4f**, and **4g**) and their respective data are presented in Table 1.


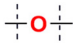
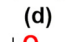
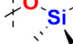
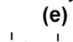
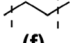
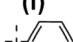
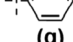
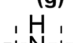
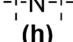


The degree of polymerization (DP_n) of **6a(d–g)** after 24 h was estimated as 5–7 units which seemed to be the expected result for these kinds of DDSQ-based linear systems.^{20,28,31,35,45} The additional reaction time (72 h) led to a minor increase in molecular weights of the obtained copolymers and their D values. Based on the analysis of molecular weight distribution plots the low molecular fractions were converted to higher molecular weight products, *e.g.* as in the case of **6a–f** – entries 4 and 5.^{30,31} This led to the question of what is the reason for such a slowdown in the course of the polymerization process? Is it caused by the Pt catalyst occluding the structure of the copolymer entangled chains resulting in its activity decrease, its deactivation, or steric hindrance and diffusion considerations? To answer this question, an independent experiment was carried out between **1a** and **4d**, performed under standard conditions. After 72 h a respective amount of [Pt₂(dvds)₃] (10^{-3} per mol of Si–H) was added and the reaction was carried out for an additional 24 h. GPC analysis showed only a minor change in the molecular weight of the resulting copolymer **6a–d** ($M_w = 7200$, DP_n = 4). This might suggest that the steric or diffusion reasons are to blame. An analogical test between **1a** and **4d** was performed and after 24 h a respective amount of [Pt₂(dvds)₃] (10^{-3} per mol of Si–H) was added along with the mixture of



Scheme 2 General synthetic procedure for alternating A–B type organic–inorganic co-oligomers with DDSQ and different organosilicon spacers *via* a hydrosilylation reaction.



Table 2 Molecular weights of co-polymers obtained *via* hydrosilylation of divinylsubstituted DDSQs (**1b** and **1c**) with dihydro-substituted organosilicon derivatives (**5d–h**)


| Entry | Sample | DDSQ |  | All fractions | | | | |
|-------|---------------------------------|--|---|---|---------|--------|--------|----|
| | | | | M_w | M_n | D | DP_n | |
| 1 | 7b-d-24h | 1b |  | 2300 | 9100 | 2.5 | 7 | |
| 2 | 7b-d-72h | | | 42 000 | 11 700 | 3.6 | 9 | |
| 3 | 7b-d-24h PtO₂ | | | 8900 | 5500 | 1.6 | 4 | |
| 4 | 7b-e-24h | | |  | 624 300 | 23 000 | 27.2 | 16 |
| 5 | 7b-e-72h | | | | 764 600 | 21 800 | 35.0 | 15 |
| 6 | 7b-f-24h | 1c |  | 4600 | 3700 | 1.2 | 3 | |
| 7 | 7b-f-72h | | | 7800 | 5200 | 1.5 | 4 | |
| 8 | 7b-g-24h | | |  | 10 600 | 5700 | 1.9 | 4 |
| 9 | 7b-g-72h | 17 700 | 9100 | | 1.9 | 7 | | |
| 10 | 7b-g-24h PtO₂ |  | 10 300 | 5600 | 1.8 | 4 | | |
| 11 | 7b-h-24h | 1c |  | 2400 | 1600 | 1.5 | 1 | |
| 12 | 7b-h-72h | | | 6800 | 2300 | 2.9 | 2 | |
| 13 | 7b-h-24h PtO₂ | | | 1400 | 1000 | 1.3 | 1 | |
| 14 | 7c-d-24h | | |  | 18 300 | 8400 | 2.2 | 6 |
| 15 | 7c-d-72h | | | | 67 000 | 15 200 | 4.4 | 10 |
| 16 | 7c-e-24h |  | 519 900 | 16 100 | 32.4 | 10 | | |
| 17 | 7c-e-72h | | 950 700 | 27 400 | 34.7 | 18 | | |
| 18 | 7c-f-24h | 1c |  | 4900 | 4200 | 1.2 | 3 | |
| 19 | 7c-f-72h | | | 105 200 | 20 200 | 5.2 | 14 | |
| 20 | 7c-g-24h | | |  | 11 200 | 6100 | 1.8 | 4 |
| 21 | 7c-g-72h | 21 200 | 8500 | | 2.5 | 6 | | |
| 22 | 7c-h-24h | 1c |  | 4500 | 3100 | 1.4 | 2 | |
| 23 | 7c-h-72h | | | 45 500 | 11 200 | 4.1 | 8 | |
| 24 | 7c-h-24h PtO₂ | | | 2000 | 1700 | 1.2 | 1 | |

Reaction conditions: $[Pt_2(dvds)_3]$ and $PtO_2 - 10^{-3}$ per mol of Si-H, equimolar stoichiometry of Si-H and Si-HC=CH₂ reagents, e.g. $[1b/c]:[5d] = 1:1$, toluene ($m_{1b/c}/V_{tot} = 33$ mg mL⁻¹), 95 °C, 24 h or 72 h. D = dispersity index, DP_n = degree of polymerization.

styrene and HSiMe₂Ph (stoichiometry 1 : 1) and the reaction was continued for an additional 24 h. After reaction completion, the resulting **6a-d** was precipitated in *n*-hexane and the decant was analysed *via* GC and GC-MS techniques. Styrene conversion was estimated as 92% after 24 h while the same reaction of styrene and HSiMe₂Ph but without the presence of co-oligomer **6a-d** enabled >99% styrene conversion in less than 8 h. In parallel, a similar test of styrene hydrosilylation by HSiMe₂Ph in the post-reaction mixture of **6a-d** was performed but without an additional amount of $[Pt_2(dvds)_3]$ after 24 h. GC analysis revealed 68% conversion of styrene (for details see the ESI, p. S-6†). These studies may confirm that $[Pt_2(dvds)_3]$ is partially occluded in the entangled chains of the copolymer **6a-d** with the rigid DDSQ units. Again, it is consistent with the Chalk-Harrod HS mechanism.²² The possibility of using PtO₂ as a catalyst known for its activity in hydrosilylation was verified.^{46,47}

But the obtained results were noticeably worse compared to those for $[Pt_2(dvds)_3]$ in terms of M_w and M_n of the obtained co-oligomers, DP_n , and main polymer fraction content (Table 1, entries 3, 6 and 9). The GPC results considering the content of all fractions presented in Table 1 are consistent with the content of the main and highest volume fraction content, presented in Table S2 (in the ESI)† in the range of 63 to 100%.

In the next step the reagents with changed Si-H and Si-Vi placement were studied in hydrosilylation, *i.e.* DDSQs with two -CH=CH₂ moieties attached directly to the DDSQ core (**1b**) or *via* the linker -OSi(Me₂)- (**1c**) with the respective dihydro-substituted organosilicon compounds (**5d-h**). The palette of dihydro-substituted reagents was extended by **5e** and **5h**, *i.e.* trisiloxane (**5e**) and disilazane (**5h**) derivatives. The respective GPC data for the obtained copolymers – type **7b** and **7c**, are presented in Table 2 and Table S2 in the ESI† with additional



information on the percentage content of the main and the highest M_w fractions.

In the cases of **1b** and **1c**, *i.e.* the DDSQ core with two $\equiv\text{Si-HC}=\text{CH}_2$ groups, hydrosilylation with dihydrosubstituted organosilicon derivatives (**5d-h**) resulted in the formation of the respective copolymers **7b** and **7c** type and was found to be dependent on the DDSQ core (**1b** and **1c**) as well as the **5d-h** co-monomer structure. The electronic impact (withdrawing or donating) of the spacer between Si-H moieties of **5d-h** could be considered in these examples. For **7b** type co-polymers, the DP_n was estimated as 3–5 units for **5f** – ethane bridged and 4–7 units for **5g** – 1,4-phenylene-bridged (both electron-donating units), regardless of the reaction time (24 *vs.* 72 h) (Table 2, entries 6–9). This is similar to the data obtained for the aforementioned **6a-f** and **6a-g** systems, analogous in the structure, but obtained from **1a** and **4f**, **4g** (reagents differing in $\equiv\text{Si-HC}=\text{CH}_2$ and Si-H placement) (Table 1, entries 4, 5 and 7, 8). Also, these results are respectively consistent with the content of the main and highest molecular weights fractions, see Table S2 (in the ESI),† entries 15–18 (in a range of 66–100%). In the case of **1c** – DDSQ with a vinyl moiety attached to the core *via* linker $-\text{OSi}(\text{Me}_2)-$, the respective copolymers **7c-f** and **7c-g** exhibited oligomeric structures with the DP_n in the range of 3–4 after 24 h and their increase was noted after 72 h, *i.e.* $DP_n = 14$ and $DP_n = 6$, respectively (Table 2, entries 18–21), with a slightly higher D index in the range of 2.5–5.2. The values of the main and highest molecular weight fractions revealed the presence of *ca.* 82% of the content of higher molecular weights of **7c-f** with $DP_n = 34$ and *ca.* 39% of **7c-g** with $DP_n = 20$ measured for samples after 72 h (Table S2,† entries 27–30). This is a significant change in the molecular weights of DDSQ copolymers obtained *via* hydrosilylation which may be attributed not only to the steric availability of the $\equiv\text{Si-HC}=\text{CH}_2$ of **1c** but also to the electronic impact of reagents.

Interestingly, the impact of the surrounding electron and steric properties of the reagents on the obtained results was visible in the case of dihydro-substituted organosilicon compounds with the presence of more electron-withdrawing moieties, *i.e.* slightly for **5d** – disiloxane and especially for **5e** – trisiloxane reacting with DDSQ-divinyl compounds, *i.e.* **1b** and **1c**. For **7b-d** and **7c** and **7d** the changes in the obtained molecular weights after 24 and 72 h were not that substantial with the DP_n in the range of 7–10. Only the separation of the highest molecular weight fractions revealed the presence of *ca.* 46% content of the fraction with $DP_n = 21$ after 24 h that changed after 72 h to *ca.* 25% content of the fraction with $DP_n = 68$ (Table S2,† entries 10 and 11). In the cases of trisiloxane **5e** and **1b**, the obtained DP_n values of **7b-e** after 24 and 72 h were higher, *i.e.* in the range of 15–16 (Table 2, entries 4 and 5). But the D index showed a significantly wider molecular weight distribution. More adequate data were obtained for the main and highest molecular weight fraction identification (Table S2,† entries 13 and 14). It revealed 40% content of the main fraction with $DP_n = 7$ after 24 h, and after 72 h there was a significant increase with $DP_n = 108$ for *ca.*

39% of the content of **7b-e**. Interestingly, the results presented for the highest molecular weight content were more impressive, with $DP_n = 1083$ after 24 h and $DP_n = 1127$ after 72 h for up to 23% sample content. What is more, the results obtained for **5e** and **1c** (with a $-\text{OSi}(\text{Me}_2)-$ linker) were even more extraordinary. Again, the DP_n for all fractions of **7b** and **7c** equalled 10 (after 24 h) and 18 (after 72 h) with substantial D values (up to 35). But the detailed data on the main molecular weight fraction of *ca.* 40% content exhibited $DP_n = 10$ (24 h) that notably increased until $DP_n = 79$ after 72 h. Considering the highest molecular weight content fractions, they were estimated as $DP_n = 1412$ after 24 h which changed to $DP_n = 1049$ with 10% and *ca.* 23% fraction contents, respectively. It should be noted that the molecular weights of copolymers **7b-e** and **7c-e** are over $2837 \times 10^3 \text{ g mol}^{-1}$ and $3927 \times 10^3 \text{ g mol}^{-1}$ and are the first examples of copolymeric A-B alternating systems with a DDSQ moiety embedded in the linear structure of the polymer with such high values of M_w . In the end, the tests of dihydrodisilazane (**5h**) with **1b** and **1c** showed that the presence of an NH moiety significantly affected its catalytic reactivity when compared to the respective disiloxane **5d**. The compounds **7b-h** and **7c-h** with $DP_n = 1-8$ revealed their lower reactivity in the process which influenced the lower molecular weights of the respective copolymers (Table 2, entries 11–13 and 22–24). This may be attributed to the possible NH coordination to the metal centre, catalyst poisoning, or disilazane degradation, *i.e.* Si-H disproportionation.^{48–50} However, for **7c-h** the molecular weights are ten times higher after 72 h (entries 22 and 23) when compared to **7b-h** and a three-fold molecular weight increase is observed after 72 h (entries 11 and 12). This may be attributed to the steric and electronic structures of substrates **1b vs.** **1c** (presence of a $-\text{SiO}(\text{Me}_2)-$ linker). It was also visible in the case of the aforementioned products **7c-e vs.** **7b-e**. Finally, in the case of the PtO_2 catalyst, the results were worse than those obtained for Karstedt's catalyst (Table 2, entries 3, 10, 13 and 24).

The presented results may suggest the electron-withdrawing impact of the siloxane unit activates Si-H and also the $\text{Si-HC}=\text{CH}_2$ moiety in the case of the DDSQ compound though only for its M type of functional Si atom, *i.e.* for **1c**. Achieving efficient copolymerization seems to be important. The respective charts of molecular weight distributions exhibiting the electronic impact of dihydro- or divinylorganosilicon compounds (**4g vs.** **5g** and **4d vs.** **5d**) are shown in Fig. 4 and 5. The impact of the DDSQ structure with or without the $-\text{OSi}(\text{Me}_2)-$ linker between the $\text{Si-HC}=\text{CH}_2$ moiety and the DDSQ core (**1b vs.** **1c**) on the results of copolymerization is depicted in the chart in Fig. 6. In the case of the D units of the Si at the DDSQ core, the effect of the steric availability of the reactive Si-H and $\text{Si-HC}=\text{CH}_2$ units may seem to exceed the electronic influence. It should also be emphasized that other effects that may have a reasonable impact on the obtained results should also be considered, *e.g.* physical effects, *i.e.* diffusion within the entangled copolymer chains, the copolymer chain rigidity, or its susceptibility to rotation.



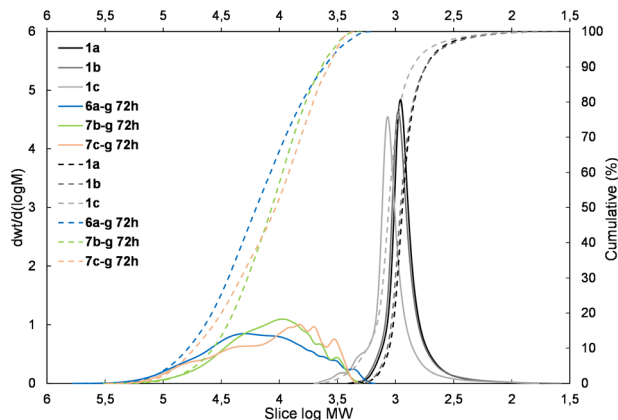


Fig. 4 The molecular weight distribution chart for copolymers obtained with 1,4-bis(dimethylsilyl)phenylene (**4g** and **5g** – electron donating moiety) – **6a–g**, **7b–g**, and **7c–g**.

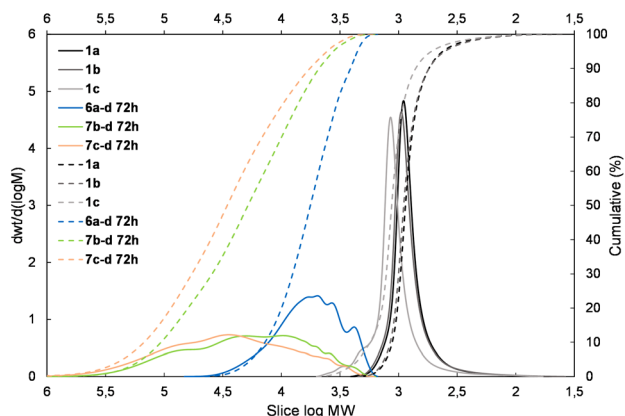


Fig. 5 The molecular weight distribution chart for copolymers obtained with the 1,1,3,3-tetramethylsiloaxane unit (**4d** and **5d** – electron-withdrawing moiety) – **6a–d**, **7b–d**, **7c–d**.

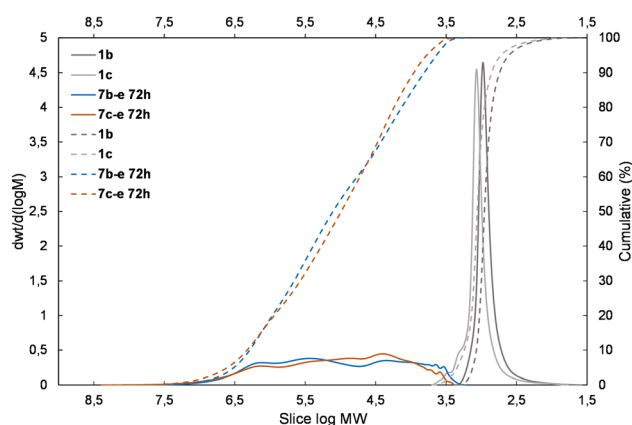


Fig. 6 The molecular weight distribution chart for copolymers of **1b** vs. **1c** obtained with the 1,1,3,3,5,5-hexamethyltrisiloaxane unit (**5e**) – **7b–e**, **7c–e**.

The results of all spectroscopic analyses for the obtained copolymers along with the GPC data presented in the respective charts are available in the ESI.†

Selected samples **7b–g** and **7c–g** were verified in terms of their solubility, especially in terms of the presence of an additional $-\text{OSi}(\text{Me}_2)-$ linker between the DDSQ core and the organosilicon spacer. As expected and reported previously, these copolymers are similarly not soluble in methanol, *n*-hexane, and acetonitrile.^{51,52}

However, in the case of dichloromethane (DCM), acetone, and tetrahydrofuran (THF) some discrepancies are observed. **7b–g** exhibited two times better solubility in DCM and is over 10-times more soluble in acetone and THF than **7c–g**. It seems that copolymers possessing $-\text{OSi}(\text{Me}_2)-$ linked to DDSQ and organosilicon fragments do not facilitate the solubility of the resulting macromolecular DDSQ-based systems (Table S4 in the ESI†). Probably the flexibility of the **7c–g** linear chain influences its increased entanglement which in turn results in solubility lowering.

Thermogravimetric analysis

The prepared silsesquioxane-containing polymers were studied by thermogravimetric analysis (TGA) to verify the influence of their structure on thermal properties. The exemplary TGA curves recorded for polymers based on the **1c** monomer are given in Fig. 7.

The results of the TGA analysis containing initial degradation temperatures ($T_d^{5\%}$ s) and the residue values at 1000 °C are provided in Table S3 in the ESI.† The performed experiments in the air atmosphere revealed that there is no simple correlation between the structure and thermal stability. In our opinion, there are too many important factors that may influence the final thermal properties of the obtained copolymers. Namely, the combination of various SQs (**1a–c**) and divinyl- or dihydrosilyl comonomers (**5d–h**, **4d–g**) have a significant impact on the polymerization process which affects the result-

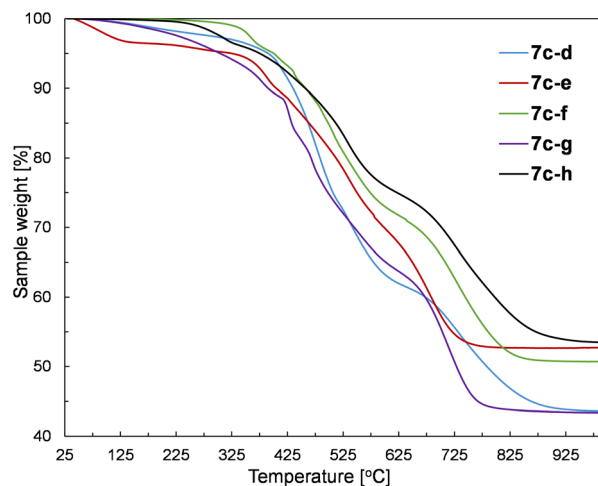


Fig. 7 TGA analysis of **7c–(d–h)** performed in air.



ing polymer parameters such as molar mass, dispersity index, and polymerization degrees. Therefore, even the polymers based on the same SQ core contain completely different mentioned-above parameters, which impedes drawing appropriate conclusions. Nevertheless, the synthesized polymers have two common features, *i.e.* the main degradation of the samples occurs at temperatures higher than 400 °C, regardless of the type of SQ core and the structure of the comonomer. Moreover, all prepared polymers revealed high residues at 1000 °C (higher than 40%), which is typical for SQ-based compounds. Furthermore, the SQ-based alkenyl monomers (**1b** and **1c**) showed to be more resistant to mass loss than the corresponding copolymers, which can be easily explained by the thermal activation of vinylsilyl-units and their subsequent polymerization/cross-linking. Therefore, the alkenyl moieties act as radical scavengers, which simply delays the degradation of the sample. This behaviour of alkenylsilsesquioxanes has already been reported.⁵³ It should be also noticed that some of the samples showed the initiation of degradation at low temperatures (below 200 °C). It could be explained by the evaporation of the solvent traces and minor low molecular weight comonomer residues that probably were occluded in the polymer chains.

Mechanical analysis

Due to the crystalline character of DDSQs³⁰ and since the resulting co-polymeric products were mostly solids (or viscous solids), we decided to measure their mechanical parameters, *i.e.* Young's modulus and hardness. Selected co-polymer films were subjected to nanomechanical research using the nanoindentation technique (described in the ESI†). Thin films of selected specimens were fabricated through spin-coating. Glass plates were cleaned with acetone and isopropanol, and a 5 wt% solution of co-polymers in DCM was deposited on them at a spin speed of 100 rpm for 40 seconds. Measurements were taken on the surface of the resulting copolymer film by evaporating the solvent at RT. The film thickness was up to 100 μm. The values of Young's modulus and Hardness are presented in Fig. 8. Unfortunately, not all prepared samples of films were suitable for the measurements. A few photographs of the selected films are presented in Fig. 9. The coatings produced have viscoelastic properties. In some of them, viscous interactions are dominant and the material flows so fast that it is not possible to perform nanoindentation measurements (especially for the compounds with an additional $-\text{OSi}(\text{Me}_2)-$ linker, *i.e.* **7c(d-h)**).

The measured values of Young's modulus varied between 2.18 and 4.48 GPa (the numerical values are presented in ESI Table S5†), and are in a few examples (entries 2 and 5, Table S5†) comparable with the results obtained for DDSQ-based linear co-oligomers with phenyl(s) spacers that we reported previously (1.81–2.67 GPa).³⁰ For other specimens, the obtained values of Young's modulus are significantly higher.²⁹ This may be attributed to the higher content of the rigid DDSQ core in the co-polymer chain in comparison with the presence of small spacers (type **d-f**). However, higher values than those

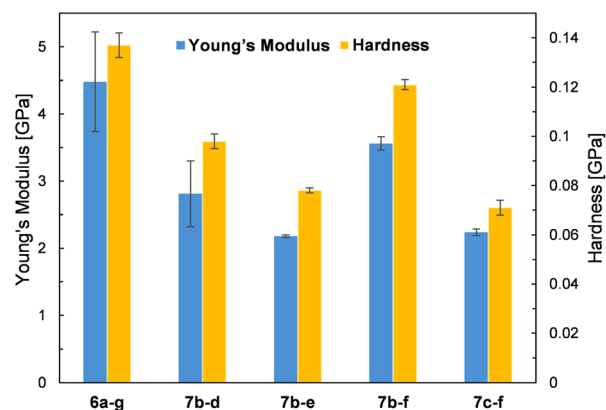


Fig. 8 Graphical presentation of Young's modulus and hardness of the analyzed samples.

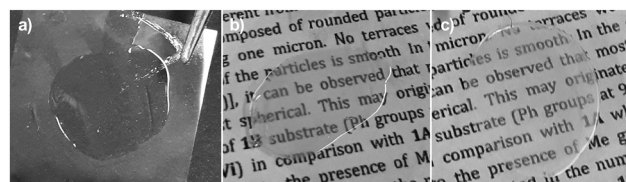


Fig. 9 Photos of selected specimens of thin films on glass plates obtained for (a) **7b-e**, (b) **7c-f**, and (c) **7c-g**.

for the respective polysiloxanes or polysilanes were observed.⁵⁴ In comparison, for selected DDSQ-based composites, *e.g.* polyurethanes modified with the DDSQ derivative, the values of Young's modulus are incomparably smaller (however, increasing with the wt% of DDSQ used) than those of DDSQ-based oligomers with the A-B type alternating building block architecture, which is justified.^{55,56} One may find a trend in changes of values for Young's modulus, *i.e.* the results obtained for systems with Si-O-Si based fragments, *e.g.* **7b-d** and **7b-e**, were lower than the values of the respective co-polymers with organic units, *i.e.* **6a-g** and **7b-f**. This analogy may be also noted in the case of hardness data. Interestingly, the compounds with an additional $-\text{OSi}(\text{Me}_2)-$ linker, *i.e.* **7c-f** exhibited a reduction of the measured values of Young's modulus and hardness.

Moreover, it was found that the surface where the film was deposited and its adhesion to it may affect the values of Young's modulus (entries 3 and 4). It will be also a subject for further detailed studies. As noted, some of the film samples prepared for **7c** type co-polymers were not suitable for the nanoindentation analysis due to their high viscosity preventing the measurement. In general, the composites and also co-polymers with the content of SQs exhibit enhanced mechanical parameters due to the intrinsic hardness of the rigid SQ segments.^{57,58}

Surface properties – static water contact angle (WCA) measurements

The effects of DDSQs embedded in the main chain of the copolymers were evaluated also through the study of their



water wettability by measurement of the static water contact angle of their thin films (prepared in the same manner as that for the nanoindentation measurements). The obtained samples in the form of colorless, transparent, or hazy films deposited on the surface of glass substrates were subjected to the WCA measurements. The selected samples are presented in Fig. 9. All of the measured samples for the 6 and 7 copolymer series exhibited contact angles in the range of 92 to 107° (see Table 3) which indicates their hydrophobic nature.

The obtained parameters undoubtedly depend on the presence (and amount) of the inorganic–organic, rigid DDSQ core, but also on the type of fragments that are linking them which is confirmed by the literature results and is also reflected herein.^{29,30,51,59–62} Nevertheless, when analyzing the obtained results, it is easy to notice that the measured water contact angle values are not only correlated with the chemical structure of materials but the quality and form of the prepared films. Water contact angle values for hazy samples oscillated between 102 and 107°, while transparent samples were characterized by lower contact angles in the range of 92 to 97°. This phenomenon should be associated with the morphology and

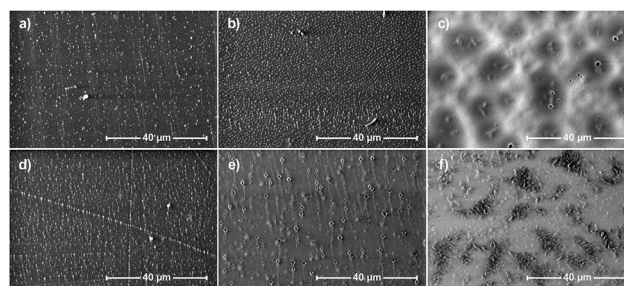


Fig. 10 Scanning electron microscopy images of samples: (a) 7b–e, (b) 7b–h, (c) 7c–d, (d) 7c–e, (e) 7c–f, and (f) 7c–g.

roughness of the surface of the obtained samples, which also affects both their appearance (transparency) and surface properties. Changes in the appearance of the obtained polymer films (see SEM images in Fig. 10(c), (e) and (f)) and their surface morphology may be the result of both differences in the chemical composition of the obtained copolymers and the resulting distinction in their physicochemical properties, *e.g.* solubility, which affect the speed and tendency to self-assemble, aggregate (Fig. 10(e) and (f)) and/or crystallize.


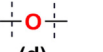
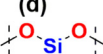
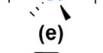
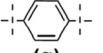
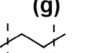
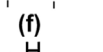
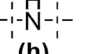
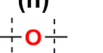
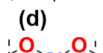
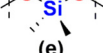
Surface morphology – SEM

To assess the effect of the discussed copolymers' chemical structures on the surface morphologies of their films selected specimens were also subjected to Scanning Electron Microscopy (SEM) imaging (Fig. 10). Samples were prepared on glass plates using 5% DCM solution using a spin coater as described before. The images of 5000× magnification were selected as the most representative. The layers obtained from samples 7b–e, 7b–h, 7c–e, 7c–d, and 7c–f are quite homogeneous. They are smooth with small holes on the surface and they originated from solvent evaporation. The average distance between the holes is much larger on sample 7c–d and is about 5 micrometres. For 7c–f, it is about 1 micrometre. The hole density on sample 7c–f is much greater than that on 7c–d, but they are about 5× smaller in diameter. Sample 7c–g is more diverse. It has smooth areas with small holes similar to 7c–f, but at the same time, about 30% of the surface is occupied by complex structures of partially ordered lamellas protruding from its surface. Single lamellas are 1–5 micrometres long and nanometric wide, and the areas containing them do not exceed 10 micrometres at a time.

Conclusions

In this work, a novel insight into the formation of linear BoC hybrid co-polymers bearing DDSQ fragments *via* hydrosilylation co-polymerization was presented. This synthetic approach was verified in terms of reactive Si–H and Si–HC=CH₂ reactive group placement in the reagents to reveal their electronic *vs.* electronic/steric impact on the degree of polymerization and molecular weight distribution of the obtained copolymers. Within conducted research, two unknown

Table 3 Water contact angle (WCA) values for glass plates coated with co-polymers (6 and 7)^a

| Sample | DDSQ |  | Film appearance | WCA [°] |
|--------|------|---|--------------------------|---------|
| 7b–d | 1b |  | Hazy ^b | 105 |
| 7b–e | 1b |  | Transparent | 95 |
| 6a–g | 1a |  | Hazy ^b | 107 |
| 7b–f | 1b |  | Transparent ^b | 98 |
| 7b–h | 1b |  | Transparent | 97 |
| 7c–d | 1c |  | Hazy | 102 |
| 7c–e | 1c |  | Transparent | 92 |
| 7c–f | 1c |  | Hazy | 103 |
| 7c–g | 1c |  | Hazy | 103 |
| 7c–h | 1c |  | Transparent | 97 |

^aThin films in one layer prepared by a spin-coating technique using 5 wt% solutions of co-polymers in DCM that were deposited on the glass plates (spin speed of 100 rpm for 40 s.). ^bSurface structure of the coating with little cracks.



XRD structures of divinylfunctionalized DDSQ were resolved. As a result, a series of linear A–B alternating macromolecular hybrid systems were obtained and characterized spectroscopically (^1H , ^{13}C , ^{29}Si NMR, FT-IR) *via* gel permeation chromatography and their thermal stability was analyzed. It is worth emphasizing that for dihydrosubstituted disiloxane and trisiloxane compounds reacting with divinylfunctionalized DDSQs (**1b** and **1c**), the resulting copolymers were characterized by a 20% fraction content of M_w between 1500 and $2200 \times 10^3 \text{ g mol}^{-1}$. This is the first reported example of BoC DDSQ-based hybrid copolymers of DP_n over 1000 units. Additionally, selected samples in the form of films obtained using a spin coater on glass plates were subjected to static water contact angle measurement as well as surface morphology measurement that revealed their hydrophobic properties. Also, the nanoindentation technique enabled the determination of mechanical parameters, *i.e.* Young's modulus and hardness. These studies exhibit a thorough synthetic approach leading to the complex verification of a series of aspects that should be taken into account while designing the formation of linear SQ-based hybrid systems. Overall, this work brings a new thought and approach to the construction of DDSQ-based BoC copolymeric hydrophobic coatings of high thermal stability for practical applications.⁶³

Author contributions

B. D. conceived the experiments and designed the study. J. D., A. M., K. M., and M. R. participated in the planning of the study and carried out the synthesis and co-wrote the paper. M. D. performed GPC measurements. R. J. performed TG analysis. M. N. was responsible for nanoindentation and SEM techniques. M. K. performed the X-ray analysis of the obtained crystals. All authors discussed the results and contributed to the interpretation of data.

Conflicts of interest

There are no conflicts to declare.

Acknowledgements

The work was supported by the National Science Centre (Poland) Project OPUS UMO 2016/23/B/ST5/00201 and grant no. POWR.03.02.00-00-1026/16 co-financed by the European Union through the European Social Fund under the Operational Program Knowledge Education Development. The authors are grateful to Mr Jan Jarożek for the project of graphical abstract.

References

- 1 D. B. Cordes, P. D. Lickiss and F. Rataboul, Recent developments in the chemistry of cubic polyhedral oligosilsesquioxanes, *Chem. Rev.*, 2010, **110**, 2081–2173.
- 2 M. Laird, N. Herrmann, N. Ramsahye, C. Totée, C. Carcel, M. Unno, J. R. Bartlett and M. Wong Chi Man, Large Polyhedral Oligomeric Silsesquioxane Cages: The Isolation of Functionalized POSS with an Unprecedented $\text{Si}_{18}\text{O}_{27}$ Core, *Angew. Chem., Int. Ed.*, 2021, **60**, 3022–3027.
- 3 K. Yoshizawa, Y. Morimoto, K. Watanabe and N. Ootake, Silsesquioxane Derivative And Process For Producing The Same, US7319129B2, 2008.
- 4 Y. Morimoto, K. Watanabe, N. Ootake, J. J. Inagaki, K. Yoshida and K. Ohguma, Silsesquioxane Derivative And Production Process For The Same, US7449539B2, 2008.
- 5 Y. Morimoto, K. Watanabe, N. Ootake, J. Inagaki, K. Yoshida and K. Ohguma, Silsesquioxane Derivatives And Process For Production Thereof, US2004/0249103A1, 2004.
- 6 *Applications of Polyhedral Oligomeric Silsesquioxanes*, ed. C. Hartmann-Thompson, Springer, London-New York, 2011.
- 7 B. Dudziec and B. Marciniak, Double-decker Silsesquioxanes : Current Chemistry and Applications, *Curr. Org. Chem.*, 2017, **21**, 2794–2813.
- 8 Q. Ye, H. Zhou and J. Xu, Cubic polyhedral oligomeric silsesquioxane based functional materials: Synthesis, assembly, and applications, *Chem. – Asian J.*, 2016, **11**, 1322–1337.
- 9 Y. Liu, X. Wu, Y. Sun and W. Xie, POSS dental nanocomposite resin: Synthesis, shrinkage, double bond conversion, hardness, and resistance properties, *Polymers*, 2018, **10**, 369–379.
- 10 R. Kunthom, P. Piyanuch, N. Wanichacheva and V. Ervithayasuporn, Cage-like silsesquioxanes bearing rhodamines as fluorescence Hg^{2+} sensors, *J. Photochem. Photobiol., A*, 2018, **356**, 248–255.
- 11 R. M. Laine, Unconventional conjugation in macromonomers and polymers, *Chem. Commun.*, 2022, **58**, 10596–10618.
- 12 H. Ghanbari, B. G. Cousins and A. M. Seifalian, A nanocage for nanomedicine: Polyhedral oligomeric silsesquioxane (POSS), *Macromol. Rapid Commun.*, 2011, **32**, 1032–1046.
- 13 C. Calabrese, C. Aprile, M. Gruttadauria and F. Giacalone, POSS nanostructures in catalysis, *Catal. Sci. Technol.*, 2020, **10**, 7415–7447.
- 14 M. Walczak, R. Januszewski, M. Dutkiewicz, A. Franczyk and B. Marciniak, A facile approach for the synthesis of novel silsesquioxanes with mixed functional groups, *New J. Chem.*, 2019, **43**, 18141–18145.
- 15 P. Żak, B. Marciniak, M. Majchrzak and C. Pietraszuk, Highly effective synthesis of vinylfunctionalised cubic silsesquioxanes, *J. Organomet. Chem.*, 2011, **696**, 887–891.
- 16 J. Duszczak, K. Mituła, R. Januszewski, P. Żak, B. Dudziec and B. Marciniak, Highly efficient route for the synthesis of a novel generation of tetraorganofunctional double-decker type of silsesquioxanes, *ChemCatChem*, 2019, **11**, 1086–1091.
- 17 K. Stefanowska, A. Franczyk, J. Szyling and J. Walkowiak, Synthesis of functional 3–buten–1–ynes and 1,3–butadienes with silsesquioxane moiety via hydrosilylation of 1,3–diynes, *ChemCatChem*, 2019, **18**, 4848–4853.



- 18 J. Kaźmierczak, K. Kuciński and G. Hreczycho, Highly Efficient Catalytic Route for the Synthesis of Functionalized Silsesquioxanes, *Inorg. Chem.*, 2017, **56**, 9337–9342.
- 19 P. Żak, B. Dudziec, M. Kubicki and B. Marciniak, Silylative Coupling versus Metathesis-Efficient Methods for the Synthesis of Difunctionalized Double-Decker Silsesquioxane Derivatives, *Chem. – Eur. J.*, 2014, **20**, 9387–9393.
- 20 J. Guan, Z. Sun, R. Ansari, Y. Liu, M. Unno, A. Ouali, S. Mahbub, J. C. Furgal, N. Yodsin, S. Jungstittiwong, D. Hashemi, J. Kieffer and R. M. Laine, Conjugated copolymers that shouldn't be, *Angew. Chem., Int. Ed.*, 2021, **60**, 11115–11119.
- 21 Y. Du and H. Liu, Cage-like Silsesquioxanes-based Hybrid Materials, *Dalton Trans.*, 2020, **49**, 5396–5405.
- 22 B. Marciniak, C. Pietraszuk, P. Pawluć and H. Maciejewski, Inorganometallics (Transition Metal-Metalloid Complexes) and Catalysis, *Chem. Rev.*, 2022, **122**, 3996–4090.
- 23 D. Troegel and J. Stohrer, Recent advances and actual challenges in late transition metal catalyzed hydrosilylation of olefins from an industrial point of view, *Coord. Chem. Rev.*, 2011, **255**, 1440–1459.
- 24 X. Du and Z. Huang, Advances in Base-Metal-Catalyzed Alkene Hydrosilylation, *ACS Catal.*, 2017, **7**, 1227–1243.
- 25 M. Zaranek and P. Pawluć, Markovnikov Hydrosilylation of Alkenes: How an Oddity Becomes the Goal, *ACS Catal.*, 2018, **8**, 9865–9876.
- 26 J. H. Jung and R. M. Laine, Beads on a Chain (BOC) Polymers Formed from the Reaction of $[\text{NH}_2\text{PhSiO}_{1.5}]_x[\text{PhSiO}_{1.5}]_{10-x}$ and $[\text{NH}_2\text{PhSiO}_{1.5}]_x[\text{PhSiO}_{1.5}]_{12-x}$ Mixtures ($x=2-4$) with the Diglycidyl Ether of Bisphenol A, *Macromolecules*, 2011, **44**, 7263–7272.
- 27 J. H. Jung, J. C. Furgal, S. Clark, M. Schwartz, K. Chou and R. M. Laine, Beads on a Chain (BoC) Polymers with Model Dendronized Beads. Copolymerization of $[(4-\text{NH}_2\text{C}_6\text{H}_4\text{SiO}_{1.5})_6(\text{IPhSiO}_{1.5})_2]$ and $[(4-\text{CH}_3\text{OC}_6\text{H}_4\text{SiO}_{1.5})_6(\text{IPhSiO}_{1.5})_2]$ with 1,4-Diethynylbenzene (DEB) Gives Through-Chain, Extended 3-D Conjugation in the Excited State That Is an Average of the Corresponding Homopolymers, *Macromolecules*, 2013, **46**, 7580–7590.
- 28 M. Seino, T. Hayakawa, Y. Ishida, M. Kakimoto, K. Watanabe and H. Oikawa, Hydrosilylation Polymerization of Double-Decker-Shaped Silsesquioxane Having Hydrosilane with Diynes, *Macromolecules*, 2006, **39**, 3473–3475.
- 29 S. Wu, T. Hayakawa, R. Kikuchi, S. J. Grunzinger, M. Kakimoto and H. Oikawa, Synthesis and Characterization of Semiaromatic Polyimides Containing POSS in Main Chain Derived from Double-Decker-Shaped Silsesquioxane, *Macromolecules*, 2007, **40**, 5698–5705.
- 30 P. Żak, B. Dudziec, M. Dutkiewicz, M. Ludwiczak, B. Marciniak and M. Nowicki, A new class of stereoregular vinylene-arylene copolymers with double-decker silsesquioxane in the main chain, *J. Polym. Sci., Part A: Polym. Chem.*, 2016, **54**, 1044–1055.
- 31 M. Walczak, R. Januszewski, M. Majchrzak, M. Kubicki, B. Dudziec and B. Marciniak, Unusual cis- and trans- architecture of dihydrofunctional double-decker shaped silsesquioxane – design and construction of its ethyl bridged π -conjugated arene derivatives, *New J. Chem.*, 2017, **41**, 3290–3296.
- 32 R. Sodkhomkhum and V. Ervithayasuporn, Synthesis of poly(siloxane/double-decker silsesquioxane) via dehydrocarbonative condensation reaction and its functionalization, *Polymer*, 2016, **86**, 113–119.
- 33 M. G. Mohamed and S. W. Kuo, Functional Silica and Carbon Nanocomposites Based on Polybenzoxazines, *Macromol. Chem. Phys.*, 2019, **220**, 1800306.
- 34 K. Tian, T. Y. Luh, X. Wang, C. Hao, X. Yang, Z. Li and G. Lai, Caterpillar-shaped polysilsesquioxanes, *Chem. Commun.*, 2019, **55**, 2613–2615.
- 35 M. Miyasaka, Y. Fujiwara, H. Kudo and T. Nishikubo, Synthesis and characterization of hyperbranched polymer consisting of silsesquioxane derivatives, *Polym. J.*, 2010, **42**, 799–803.
- 36 M. Soldatov and H. Liu, Hybrid porous polymers based on cage-like organosiloxanes: synthesis, properties and applications, *Prog. Polym. Sci.*, 2021, **119**, 101419.
- 37 Q. Ge and H. Liu, Rational design and preparation of superhydrophobic photo-cured hybrid epoxy coating modified by fluorocarbon substituted silsesquioxane-based nanoparticles, *Prog. Org. Coat.*, 2022, **172**, 107089.
- 38 F. Chen, F. Lin, Q. Zhang, R. Cai, Y. Wu and X. Ma, Polyhedral Oligomeric Silsesquioxane Hybrid Polymers: Well-Defined Architectural Design and Potential Functional Applications, *Macromol. Rapid Commun.*, 2019, **40**, 1900101.
- 39 T. Hamada, Y. Nakanishi, K. Okada, S. Tsukada, A. Uedono and J. Ohshita, Thermal Insulating Property of Silsesquioxane Hybrid Film Induced by Intramolecular Void Spaces, *ACS Appl. Polym. Mater.*, 2021, **3**, 3383–3391.
- 40 S. Tsukada, Y. Nakanishi, T. Hamada, K. Okada, S. Mineoi and J. Ohshita, Ethylene-bridged polysilsesquioxane/hollow silica particle hybrid film for thermal insulation material, *RSC Adv.*, 2021, **11**, 24968–24975.
- 41 H. Shi, J. Yang, M. You, Z. Li and C. He, Polyhedral Oligomeric Silsesquioxanes (POSS)-Based Hybrid Soft Gels: Molecular Design, Material Advantages, and Emerging Applications, *ACS Mater. Lett.*, 2020, **2**, 296–316.
- 42 P. Żak, M. Majchrzak, G. Wilkowski, B. Dudziec, M. Dutkiewicz, B. Marciniak, P. Żak, M. Majchrzak, G. Wilkowski, B. Dudziec, M. Dutkiewicz and B. Marciniak, Synthesis and characterization of functionalized molecular and macromolecular double-decker silsesquioxane systems, *RSC Adv.*, 2016, **6**, 10054–10063.
- 43 D. Brząkalski, M. Walczak, J. Duszczak, B. Dudziec and B. Marciniak, Chlorine-Free Catalytic Formation of Silsesquioxanes with Si-OH and Si-OR Functional Groups, *Eur. J. Inorg. Chem.*, 2018, **45**, 4905–4910.
- 44 A. Władczyn, A. Gağor, K. Ślepokura and Ł. John, Hydroxyalkyl-substituted double-decker silsesquioxanes: effective separation of cis and trans isomers, *Inorg. Chem. Front.*, 2022, **9**, 3999–4008.



- 45 J. Guan, Z. Zhang and R. M. Laine, Synthesis and Characterization of Rigid-Rod Polymers with Silsesquioxanes in the Main Chain, *Macromolecules*, 2022, **55**, 5403–5411.
- 46 K. Stefanowska, A. Franczyk, J. Szyling, M. Pyziak, P. Pawluć and J. Walkowiak, Selective hydrosilylation of alkynes with octaspherosilicate (HSiMe₂O)₈Si₈O₁₂, *Chem. – Asian J.*, 2018, **13**, 2101–2108.
- 47 N. Sabourault, G. Mignani, A. Wagner and C. Mioskowski, Platinum oxide (PtO₂): A potent hydrosilylation catalyst, *Org. Lett.*, 2002, **4**, 2117–2119.
- 48 J. Olejarka, A. Łącz, Z. Olejniczak and M. Hasik, Non-porous and porous materials prepared by cross-linking of polyhydromethylsiloxane with silazane compounds, *Eur. Polym. J.*, 2018, **99**, 150–164.
- 49 M. Walczak, A. Franczyk and B. Marciniak, Synthesis of Monofunctionalized Silsesquioxanes (RSiMe₂O)(iBu)₇Si₈O₁₂ via Alkene Hydrosilylation, *Chem. – Asian J.*, 2018, **13**, 181–186.
- 50 C.-W. Chen, H. Yu, M.-Y. Huang and Y.-Y. Jiang, Hydrogenation of m-Xylene Catalyzed by a Silica-supported Polysilazane-Platinum Complex, *Polym. Adv. Technol.*, 1996, **7**, 79–83.
- 51 J. Xu, W. Zhang, Q. Jiang, J. Mu and Z. Jiang, Synthesis and properties of poly(aryl ether sulfone)s incorporating cage and linear organosiloxane in the backbones, *Polymer*, 2015, **62**, 77–85.
- 52 J. Hao, Y. Wei, X. Li and J. Mu, Poly(arylene ether ketone)s with low dielectric constants derived from polyhedral oligomeric silsesquioxane and difluorinated aromatic ketones, *J. Appl. Polym. Sci.*, 2018, **135**(15), 46084.
- 53 J. Duszczak, K. Mituła, A. Santiago-Portillo, L. Soumoy, M. Rzonsowska, R. Januszewski, L. Fusaro, C. Aprile and B. Dudziec, Double-Decker Silsesquioxanes Self-Assembled in One-Dimensional Coordination Polymeric Nano fibers with Emission Properties, *ACS Appl. Mater. Interfaces*, 2021, **13**, 22806–22818.
- 54 E. Yilgör and I. Yilgör, Silicone containing copolymers: Synthesis, properties and applications, *Prog. Polym. Sci.*, 2014, **39**, 1165–1195.
- 55 B. Zhao, K. Wei, L. Wang and S. Zheng, Poly(hydroxyl urethane)s with Double Decker Silsesquioxanes in the Main Chains: Synthesis, Shape Recovery, and Reprocessing Properties, *Macromolecules*, 2020, **53**, 434–444.
- 56 B. Zhao, H. Ding, S. Xu and S. Zheng, Organic–Inorganic Linear Segmented Polyurethanes Simultaneously Having Shape Recovery and Self-Healing Properties, *ACS Appl. Polym. Mater.*, 2019, **1**, 3174–3184.
- 57 A. M. Díez-Pascual, M. A. Gómez-Fatou, F. Ania and A. Flores, Nanoindentation in polymer nanocomposites, *Prog. Mater. Sci.*, 2015, **67**, 1–94.
- 58 M. Wang, H. Chi, K. S. Joshy and F. Wang, Progress in the Synthesis of Bifunctionalized Polyhedral Oligomeric Silsesquioxane, *Polymers*, 2019, **11**, 2098–2118.
- 59 S. Wu, T. Hayakawa, M. A. Kakimoto and H. Oikawa, Synthesis and characterization of organosoluble aromatic polyimides containing POSS in main chain derived from double-decker-shaped silsesquioxane, *Macromolecules*, 2008, **40**, 5698–5705.
- 60 K. Wei, L. Wang and S. Zheng, Organic-inorganic copolymers with double-decker silsesquioxane in the main chains by polymerization via click chemistry, *J. Polym. Sci., Part A: Polym. Chem.*, 2013, **51**, 4221–4232.
- 61 W. Zhang, J. Xu, X. Li, G. Song and J. Mu, Preparation, characterization, and properties of poly(aryl ether sulfone) systems with double-decker silsesquioxane in the main chains by reactive blending, *J. Polym. Sci., Part A: Polym. Chem.*, 2014, **52**, 780–788.
- 62 L. Wang, C. Zhang and S. Zheng, Organic-inorganic poly(hydroxyether of bisphenol A) copolymers with double-decker silsesquioxane in the main chains, *J. Mater. Chem.*, 2011, **21**, 19344–19352.
- 63 Z. Zhang, J. Guan, R. Ansari, J. Kieffer, N. Yodsinn, S. Jungstittiwong and R. M. Laine, Further Proof of Unconventional Conjugation via Disiloxane Bonds: Double Decker Sesquioxane [vinylMeSi(O_{0.5})₂(PhSiO_{1.5})₈(O_{0.5})₂SiMevinyl] Derived Alternating Terpolymers Give Excited-State Conjugation Averaging That of the Corresponding Copolymers, *Macromolecules*, 2022, **55**, 8106–8116.

